

1 **Ocean liming effects on dissolved organic matter dynamics**

2

3 Chiara Santinelli¹, Silvia Valsecchi^{1,2,3}, Simona Retelletti Brogi^{1,4}, Giancarlo Bachi¹, Giovanni
4 Checcucci¹, Mirco Guerrazzi¹, Elisa Camatti⁵, Stefano Caserini^{3,6}, Arianna Azzellino^{2,3}, Daniela
5 Basso^{3,7}

6

7

1 Consiglio Nazionale delle Ricerche (CNR), Istituto di Biofisica. Via Moruzzi 1, 56124 Pisa (PI), Italia.

8

2 Politecnico di Milano, Dipartimento di Ingegneria Civile ed Ambientale. Piazza Leonardo da Vinci 32, 20133 Milano (MI), Italia.

9

3 Consorzio Nazionale Interuniversitario per le Scienze del Mare (CoNISMa). Piazzale Flaminio 9, 00196 Roma (RM), Italia.

10

4 Istituto di Oceanografia e Geofisica Sperimentale (OGS), Sezione di Oceanografia. Via Piccard 54, 34151 Trieste (TS), Italia.

11

5 Consiglio Nazionale delle Ricerche (CNR), Istituto di Scienze Marine. Arsenale Tesa 104, Castello 2737/F - 30122 Venezia (VE), Italia.

12

6 Università di Parma, Dipartimento di Ingegneria e Architettura. Parco Area delle Scienze 181/A, 43124 Parma (PR), Italia.

13

7 Università degli Studi di Milano-Bicocca, Dipartimento di Scienze dell'ambiente e della terra. Piazza della Scienza 4, 20126 Milano (MI), Italia.

14

15

16

Correspondence to: Chiara Santinelli (chiara.santinelli@ibf.cnr.it)

17

18 **Abstract.** Ocean liming has gained attention as a potential solution to mitigate climate change by actively removing
19 carbon dioxide (CO₂) from the atmosphere. The addition of hydrated lime into oceanic surface water leads to an increase
20 in alkalinity, which in turn promotes the uptake and sequestration of atmospheric CO₂.
21 Despite the potential of this technique, its effects on the marine ecosystem are still far to be understood, and there is
22 currently no information on the potential impacts on the concentration and quality of Dissolved Organic Matter (DOM),
23 that is one of the largest, the most complex and yet the least understood mixture of organic molecules on Earth.
24 The aim of this study is to provide the first experimental evidence about the potential effects of hydrated lime addition on
25 DOM dynamics in the oceans, by assessing changes in its concentration and optical properties (absorption and
26 fluorescence).
27 To investigate the effects of liming on DOM pools with different concentrations and quality, seawater was collected from
28 two contrasting environments: the oligotrophic Mediterranean Sea, known for its Dissolved Organic Carbon (DOC)
29 concentration comparable to that observed in the oceans, and the eutrophic Baltic Sea, characterized by high DOM
30 concentration mostly of terrestrial origin. hydrated lime was added in both waters, to reach a pH of 9 and 10.
31 Our findings reveal that the addition of hydrated lime has a noticeable effect on DOM dynamics in both the Mediterranean
32 Sea and Baltic Sea, determining a reduction in DOC concentration and a change in the optical properties (absorption and
33 fluorescence) of DOM. These effects, detectable at pH 9, become significant at pH 10 and are more pronounced in the
34 Mediterranean Sea than in the Baltic Sea. These potential short-term effects should be considered within the context of
35 the physico-chemical properties of seawater and the seasonal variability.

36 **1 Introduction**

37 Oceans are a natural sink for atmospheric CO₂ having the potential to mitigate its increase and therefore the effects of
38 climate change (Gattuso et al., 2013; Heinze et al., 2015). The massive amount of atmospheric CO₂ absorbed by the
39 oceans in the last decades (~ 30-40% of anthropogenic emissions), is generating dramatic global-scale changes in seawater
40 chemistry, such as a decrease in pH, in carbonate concentration and in the ocean buffering capacity (Chikamoto et al.,
41 2023). Even if the ongoing efforts toward a global reduction of anthropogenic CO₂ emissions should be rapidly intensified,
42 the available projections highlight the need for additional strategies, such as the development of efficient ocean-based
43 Negative Emission Technologies (NETs) (Calvin et al., 2023; Royal Society and Royal Academy of Engineering, 2018).
44 Some NETs are not only capable of removing atmospheric CO₂ and store it as bicarbonate ions into the oceans, but also
45 of increasing the water pH, restoring ocean buffering capacity to the pre-industrial era (Butenschön et al., 2021; Gore et
46 al., 2019). One of these NETs is Ocean Alkalinity Enhancement (OAE) (also called Artificial Ocean Alkalinization,
47 AOA), which relies on the dissolution of alkaline minerals such as hydrated lime (calcium hydroxide, Ca(OH)₂) into the
48 oceans) (Kheshgi, 1995). Although the exact amount of hydrated lime to be released, as well as its sparging methods, is
49 still under debate one of the proposals is to discharge highly concentrated slurry (*lime milk*) from large cargo ships, tankers
50 and/or dedicated vessels. Caserini et al., (2021) simulated the pH dynamics within the wake of a sparging ship releasing
51 Ca(OH)₂ with an initial particle radius of 45 μm at a rate of 10 kg s⁻¹. The results of their modeling study suggest that in
52 these conditions a temporary, sharp increase in pH of about 1 unit can be observed at the discharge site, and that the
53 effects decrease moving far from the discharge site, becoming lower than 0.2 pH units at a distance of 1400 – 1600 m
54 (0.8-0.9 nautical miles).

55 The discharge of alkaline minerals may trigger the inorganic precipitation of calcium carbonate (CaCO₃), reducing the
56 efficiency of the CO₂ sink and negatively affecting seawater transparency and photosynthetic rates (González and Ilyina,
57 2016), with possible consequences for the biogeochemical cycles and the functioning of the marine ecosystem (Camatti
58 et al., 2024). The side effects of OAE techniques on the marine environment need to be thoroughly investigated before
59 making any decision on their use. To the best of our knowledge, there is no information on the effects that ocean liming
60 may have on Dissolved Organic Matter (DOM) and its chromophoric fraction (CDOM, i.e. the light-absorbing fraction
61 and FDOM, i.e. its fluorescent fraction). Holding an amount of carbon of 660 billion metric tons and being the most
62 concentrated dissolved component in the oceans (Hansell et al., 2009), every action that could modify seawater chemistry
63 is expected to have an impact on this key component of the carbon cycle. DOM represents the main source of energy for
64 heterotrophic prokaryotes, a change in its concentration and/or quality could therefore have a cascading effect on the
65 functioning of marine ecosystem.

66 The aim of this study is to provide the first experimental evidence about the potential effects of hydrated lime addition on
67 DOM dynamics in the oceans, by assessing changes in its concentration and optical properties (absorption and
68 fluorescence). In order to investigate the impact on DOM pool with different origin and optical properties, seawater was
69 collected from two highly diverse environments; (1) the oligotrophic Mediterranean Sea, characterized by Dissolved
70 Organic Carbon (DOC) concentration comparable to those observed in the open oceans, and (2) the eutrophic Baltic Sea,
71 characterized by high DOC concentration, mostly of terrestrial origin.

72

73 2 Materials and methods

74 In order to investigate the effects of ocean liming on DOM dynamics, an ultra-pure $\text{Ca}(\text{OH})_2$ powder was added to natural
75 seawater and changes in DOC concentration, absorption and fluorescence of CDOM were followed for 24 hours at the
76 laboratories of the Biophysics Institute, CNR (Pisa, Italy). Based on the results by Caserini et al. (2021), which suggested
77 a sharp increase of 1 unit of pH at the discharge site of a sparging ship, the experiment was carried out at pH 9. Although
78 unlikely under actual conditions of dilution in the open sea, an additional experiment was carried out at pH 10 because
79 this situation may occur in coastal waters (e.g. coastal lagoons, high primary productivity enhanced by eutrophication)
80 (Hinga, 2002). $\text{Ca}(\text{OH})_2$ was provided by UNICALCE (Sedrina (BG), Italy) and supplied as powder (Tab. S1). Seawater
81 was collected at Marina di Pisa, Tyrrhenian Sea, Italy (Mediterranean Sea) and in the coastal area surrounding Riga,
82 Latvia (Baltic Sea) (Tab. 1).

	Sampling Date	Salinity	pH	DOC (μM)	a_{254} (m^{-1})	$S_{275-295}$ (nm^{-1})
Mediterranean Sea	Mar-22	38	8.2	66 ± 0.5	1.9	0.024
Baltic Sea	Apr-22	6	8.1	364 ± 3	24.5	0.021

83 **Table 1: Chemical and physical properties of the Mediterranean Sea and Baltic Sea water used for the**
84 **experiment.**

85

86 2.1 Experimental setup

87 In order to investigate the impact of slaked lime on chemical-physical processes affecting DOM dynamics, seawater was
88 sterilized by filtration through a 0.2 μm pore size filter (Polycap AS36 filter capsule, Whatman, UK) using a peristaltic
89 pump (Masterflex™ L/S™, Germany). Salinity was measured by using a HI 9033 portable probe (Hanna Instruments,
90 USA). The experiments were carried out in 2 L acid-washed polycarbonate®Nalgene bottles as follows:

91 1. Mediterranean Sea

- 92 a. Treatment: filtered surface seawater enriched with $\text{Ca}(\text{OH})_2$ powder to reach:
- 93 • pH 9, $[\text{Ca}(\text{OH})_2]$ 0.04 g/L
 - 94 • pH 10, $[\text{Ca}(\text{OH})_2]$ 0.25 g/L
- 95 b. Control: filtered surface seawater (pH = 8.2)

96 2. Baltic Sea

- 97 a. Treatment: filtered surface seawater enriched with $\text{Ca}(\text{OH})_2$ powder to reach
- 98 ▪ pH of 9, $[\text{Ca}(\text{OH})_2]$ 0.01 g/L
 - 99 ▪ pH 10, $[\text{Ca}(\text{OH})_2]$ 0.06 g/L
- 100 b. Control: filtered surface seawater (pH = 8.1)

101 All the experiments were carried out in triplicates and the bottles were stored in the dark and at room temperature ($22 \pm$
102 1 °C). Immediately after the addition of the $\text{Ca}(\text{OH})_2$ powder, the bottles were gently mixed. Before and after powder
103 addition and before each sampling time, pH was measured using an edge HI2002-02 pH-meter (Hanna Instruments, USA).

104 In the treatment at pH 9, the pH slightly decreased by 0.06 (Baltic Sea) and 0.29 (Mediterranean Sea) between 3 and 22
105 h after the addition (Tab. S2). In the treatment at pH 10, 3 hours after the addition the pH decreased by 0.3 in the
106 Mediterranean Sea and after 22 hours it decreased by 0.45 in the Mediterranean Sea and 0.26 in the Baltic Sea (Tab. S2).
107 Subsamples for DOC (40 mL) and CDOM/FDOM (60 mL) analyses were collected before Ca(OH)₂ addition and 5', 30',
108 3 h and 22 h after Ca(OH)₂ addition.

109 The bottles were gently mixed before subsampling at 5', 30', and 3 h. After 22 hours, carbonate sedimentation was clearly
110 visible at the bottom of the bottles, samples of the supernatant were therefore collected before mixing for both DOC and
111 CDOM/FDOM analyses, and an additional sample was collected after gently mixing only for DOC analyses since
112 CDOM/FDOM would have been strongly affected by the scattering due to the suspended particles.

113 Samples for CDOM/FDOM analyses were brought to pH 7.5 ± 1.0 with high purity 2 M HCl, to avoid the effect of pH
114 on DOM absorption and fluorescence and filtered through a PES 0.2 μm pore size syringe filter (Minisart 16534K,
115 Sartorius, Germany), to avoid the scattering due to the presence of carbonate particles in solution.

116

117 **2.2 DOC**

118 Samples for DOC analyses were acidified at pH 2 with high purity 2 M HCl. DOC measurements were carried out with
119 a TOC-L analyzer (Shimadzu, Japan), by high temperature catalytic oxidation following Santinelli et al. (2015). Samples
120 were sparged for 3 min with CO₂-free ultrahigh purity nitrogen to remove inorganic carbon. 150 μL of the sample were
121 injected into the furnace after a three-fold rinsing with the sample to be analyzed. From 3 to 5 replicate injections were
122 performed until the analytical error was lower than 1%. A four-point calibration curve was measured using a standard
123 solution of potassium hydrogen phthalate in the same concentration range as the samples. The system blank was measured
124 every day at the beginning and the end of the analyses using low-carbon water (2-3 $\mu\text{M C}$). The instrument performance
125 was verified daily using the DOC Consensus Reference Material (CRM) (Hansell, 2005) (CRM Batch #20/08-20, nominal
126 concentration of $42 \pm 1 \mu\text{M}$; measured concentration $40 \pm 2 \mu\text{M}$, 76 CRM samples analyzed).

127

128 **2.3 CDOM optical properties**

129 **2.3.1 Absorption**

130 Absorption spectra were measured between 230 and 700 nm with a UV-Vis spectrophotometer (Mod-7850, Jasco, USA),
131 using a 10 cm quartz cuvette. The absorption spectrum of Milli-Q water was subtracted from each sample spectrum. The
132 absorption coefficient at 254 nm (a_{254}) and the spectral slope between 275 and 295 nm ($S_{275-295}$) were calculated from the
133 absorption spectra using the ASFit tool (Omanović et al., 2019). a_{254} is used to have semi-quantitative information on
134 CDOM, since primary CDOM absorption is caused by conjugated systems having the absorption peak near 254 nm (Del
135 Vecchio and Blough, 2004; Weishaar et al., 2003). $S_{275-295}$ can be related to changes in the average aromaticity and
136 molecular weight of the molecules in the CDOM pool (Helms et al., 2008). The absorption coefficient at 280 nm and 325
137 nm (a_{280} , a_{325}) and the spectral slope ratio (Sr, ratio between $S_{275-295}$ and $S_{350-400}$) are also reported for comparison (Tab,
138 S2), being among the most used CDOM indices in the literature.

139 2.3.2 Fluorescence

140 Fluorescence excitation-emission matrices (EEMs) were recorded with an Aqualog fluorometer (Horiba-Jobin Yvon,
141 UK), using a 1 cm quartz cuvette. Excitation ranged between 250 and 450 nm at 5 nm increments; emission was recorded
142 between 212 and 619 nm at 3 nm increments. The EEMs were processed using the TreatEEM software (Omanović et al.,
143 2023). EEMs were corrected for instrumental bias in excitation and emission, and Rayleigh and Raman scatter peaks were
144 removed using the monotone cubic interpolation (shape-preserving). EEMs were normalized to the water Raman signal,
145 dividing the fluorescence by the integrated Raman band of Milli-Q water ($\lambda_{\text{ex}} = 350$ nm, $\lambda_{\text{em}} = 371$ -428 nm; Lawaetz and
146 Stedmon, 2009) measured on the same day of the analyses. The fluorescence intensity is therefore reported as equivalent
147 to water Raman Units (R.U.).

148 Parallel factor analysis (PARAFAC) was separately applied to the Mediterranean Sea and Baltic Sea samples (number
149 of EEMs: 45 for each experiment), using the decomposition routines of the EEMs toolbox for MATLAB software
150 (drEEM) (Murphy et al., 2013). The PARAFAC validated a 3-component model for both the Mediterranean Sea and the
151 Baltic Sea (Fig. S1 and S2). OpenFluor, an online database of environmental fluorescence spectra, was used as a validation
152 tool to characterize the three components (Tab. S3 and S4). OpenFluor compares excitation and emission spectra of the
153 validated components with all the components present in the database and allows comparing the spectra using the Tucker
154 Congruence Coefficient (TCC; Murphy et al. (2014)).

155

156 2.4 Statistical analyses

157 For all parameters, differences were tested using the Kruskal–Wallis nonparametric test and were considered significant
158 at the threshold of $p < 0.05$. All statistical analyses were performed using OriginPro version 9 (OriginLab, USA).

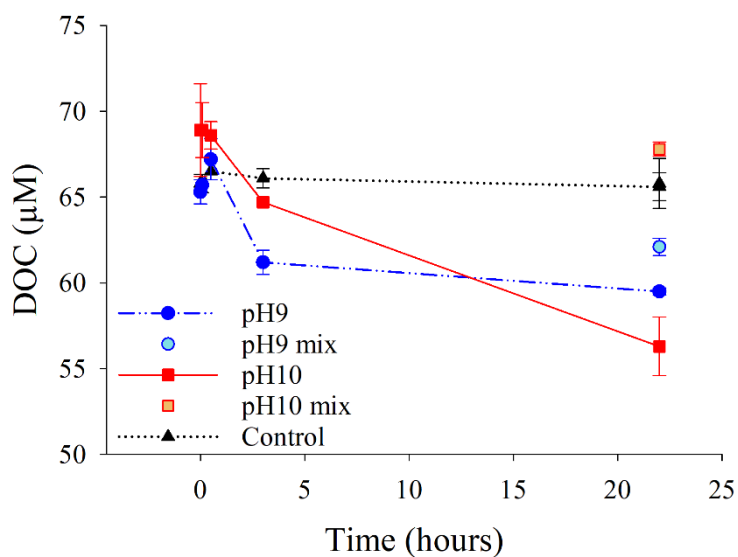
159

160 3. Results

161 3.1 Mediterranean Sea

162 3.1.1 DOC

163 In the Mediterranean Sea, three hours after $\text{Ca}(\text{OH})_2$ addition, a $4 \mu\text{M}$ (6%) DOC decrease was observed in both treatments
164 (Fig. 1, Tab. S2). A further decrease was observed in the supernatant of the unmixed sample 22 h after the addition, with
165 DOC reaching $59.5 \pm 0.1 \mu\text{M}$ (9% decrease) at pH 9 and $56.3 \pm 1.7 \mu\text{M}$ (18% decrease) at pH 10 (Tab. S2). It is noteworthy
166 that such a decline was only observed in the unmixed samples, whereas no significant change was observed in the mixed
167 samples 22 h after the addition (Fig.1, Tab. S2)



168

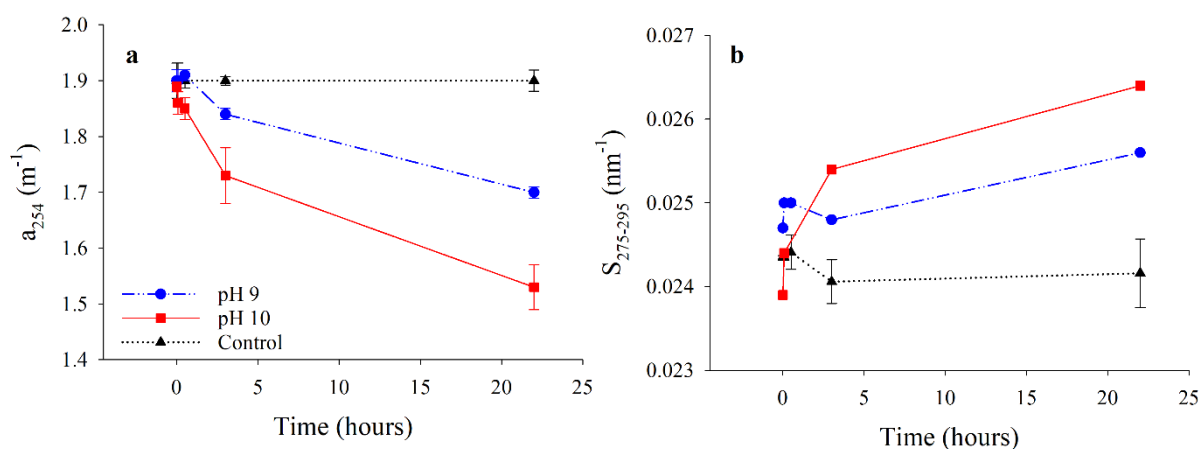
169 **Figure 1: Trend of DOC concentration in the Mediterranean Sea treatments at pH 9 and 10, and in the control.**
 170 **Error bars refer to the standard deviation among the 3 replicates. Please, note that for some samples the error**
 171 **bars are smaller than the symbols and therefore not visible.**

172

173

174 3.1.2 CDOM Absorption

175 A slight decrease in a_{254} was observed 3 hours after $\text{Ca}(\text{OH})_2$ addition at both pH (9 and 10). Interestingly, 22 h after the
 176 addition, in the supernatant of unmixed bottles, a marked decrease of 0.2 m^{-1} (10%) and 0.4 m^{-1} (19%) was observed (Fig.
 177 2a, Tab. S2) together with an increase in $S_{275-295}$ from 0.0247 nm^{-1} to 0.0256 nm^{-1} (4%) and from 0.0239 to 0.0264 nm^{-1}
 178 (10%) at pH 9 and 10, respectively (Fig. 2b, Tab. S2). Mixed samples were not collected for CDOM analyses, since
 179 scattering due to the particles would have affected the results.



180

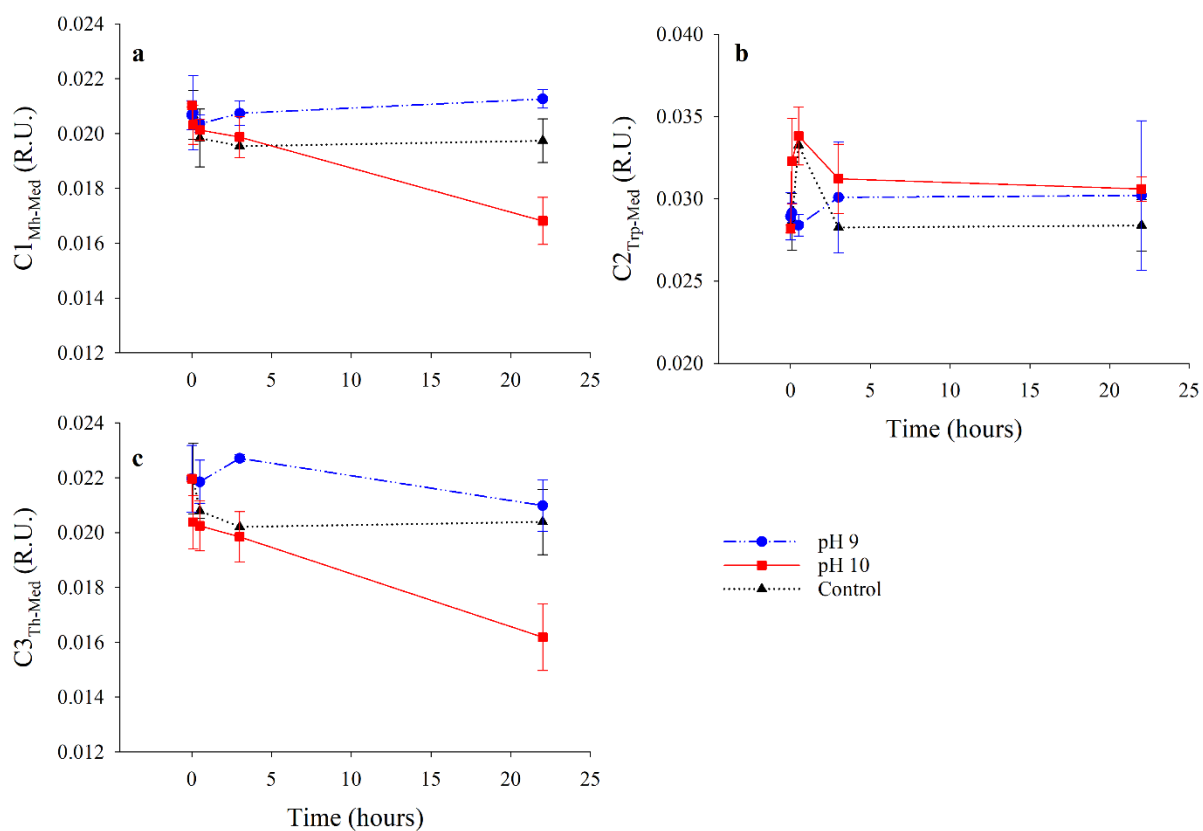
181 **Figure 2: Trend of a_{254} (a) and $S_{275-295}$ (b) in the Mediterranean Sea treatments at pH 9 and 10, and in the**
 182 **control. Error bars refer to the standard deviation among the 3 replicates. Please, note that for some samples the**
 183 **error bars are smaller than the symbols and therefore not visible.**

184

185

186 **3.1.3 FDOM fluorescence**

187 The PARAFAC validated a 3-component model for the Mediterranean Sea EEMs (Fig. S1, Tab. S3). Component 1
 188 ($\lambda_{Ex}/\lambda_{Em}$: 315/409 nm, Fig. S1a) shows spectroscopic characteristics similar to Coble's peak M ($\lambda_{Ex}/\lambda_{Em}$: 312/[380]420;
 189 Coble (1996)). The comparison with similar components in the OpenFluor database (matches with a TCC > 0.95) allowed
 190 to characterize it as marine humic-like ($C1_{Mh-Med}$). Component 2 ($\lambda_{Ex}/\lambda_{Em}$: 275/331 nm, Fig. S1b) shows spectroscopic
 191 characteristics similar to Coble's peak T ($\lambda_{Ex}/\lambda_{Em}$: 275/340 nm; Coble (1996)). The comparison with similar components
 192 in the OpenFluor database (matches with a TCC > 0.95) allowed to characterize it as tryptophan-like ($C2_{Trp-Med}$).
 193 Component 3 ($\lambda_{Ex}/\lambda_{Em}$: 260/[380]456 nm, Fig. S1c) shows spectroscopic characteristics similar to Coble's peaks C and A
 194 ($\lambda_{Ex}/\lambda_{Em}$: 350/451 and 245/451 nm, respectively; Coble (1996)). The comparison with similar components in the
 195 OpenFluor database (matches with a TCC > 0.95) allowed to characterize it as terrestrial humic-like ($C3_{Th-Med}$).
 196 $C1_{Mh-Med}$ did not show significant changes over the incubation time at pH 9 and in the control (Fig. 3a, Tab. S5). At pH
 197 10, a decrease of 0.004 R.U. (20%) was observed 22 h after the addition. $C2_{Trp-Med}$ did not show significant changes during
 198 the incubation, neither in the treatments nor in the control (Fig. 3b, Tab. S5). $C3_{Th-Med}$ showed variations only at pH 10
 199 (Fig. 3c, Tab. S5), with a slight decrease 3 hours after the addition, and a significant decrease of 0.006 R.U. (26%) at the
 200 end of the incubation (22 h).



201

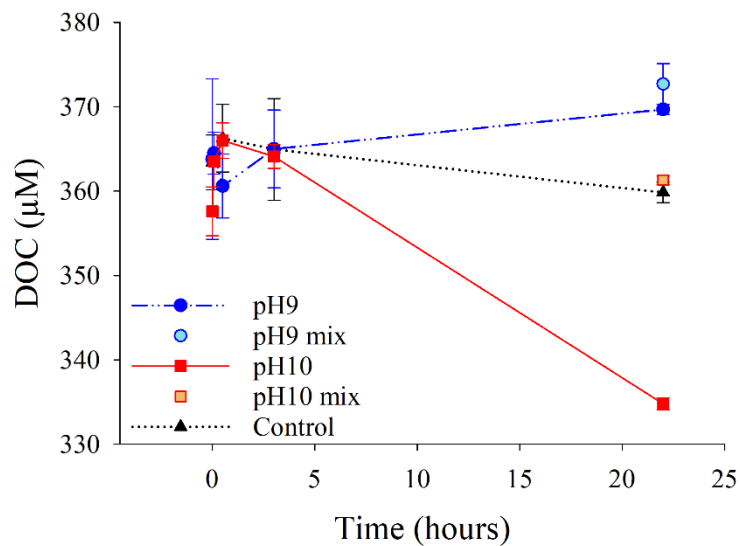
202 **Figure 3: Trend of the fluorescent intensity of C1_{Mh-Med} (a), C2_{Trp-Med} (b) and C3_{Th-Med} (c) in the Mediterranean**
 203 **Sea treatments at pH 9 and 10, and in the control. Error bars refer to the standard deviation among the 3**
 204 **replicates.**

205

206 3.2 Baltic Sea

207 3.2.1 DOC

208 In the Baltic Sea no significant change was observed 3 hours after $\text{Ca}(\text{OH})_2$ addition in both treatments (pH 9 and 10)
209 (Fig. 4, Tab. S2). At the end of the experiment (22 h), DOC decreased by $23 \mu\text{M}$ (6 %) at pH 10, whereas no significant
210 change was observed at pH 9. It is noteworthy that DOC showed significant differences between the mixed and unmixed
211 samples at pH 10, whereas in the mixed samples DOC was similar to the control (Fig. 4, Tab. S2).



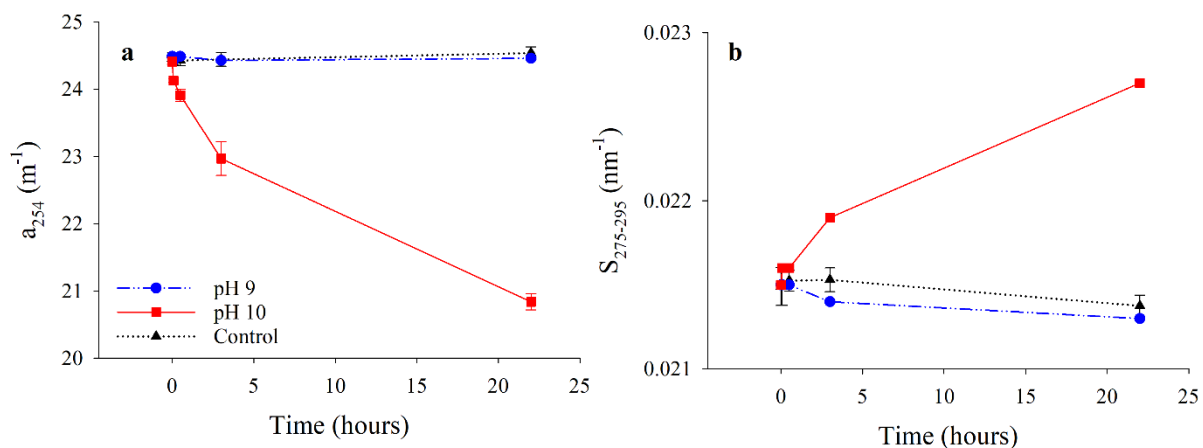
212

213 **Figure 4: Trend of DOC concentration in the Baltic Sea treatments at pH 9 and 10 and in the control. Error bars**
214 **refer to the standard deviation among the 3 replicates. Please, note that for some samples the error bars are**
215 **smaller than the symbols and therefore not visible.**

216

217 3.2.2 CDOM absorption

218 Twenty-two hours after the addition of $\text{Ca}(\text{OH})_2$, a_{254} decreased by 0.03 m^{-1} (0.1%), and 3.6 m^{-1} (15%) at pH 9 and pH
219 10, respectively (Fig. 5a). $S_{275-295}$ increased from 0.0215 nm^{-1} to 0.0227 nm^{-1} (6%) at pH 10, whereas no significant
220 change was observed at pH 9 (Fig. 5b). The change in CDOM is therefore visible only at pH 10 (Fig. 5)



221

222 **Figure 5: Trend of a_{254} (a) and $S_{275-295}$ (b) in the Baltic Sea treatments at pH 9 and 10, and in the control. Error**
 223 **bars refer to the standard deviation among the 3 replicates. Please, note that for some samples the error bars are**
 224 **smaller than the symbols and therefore not visible.**

225

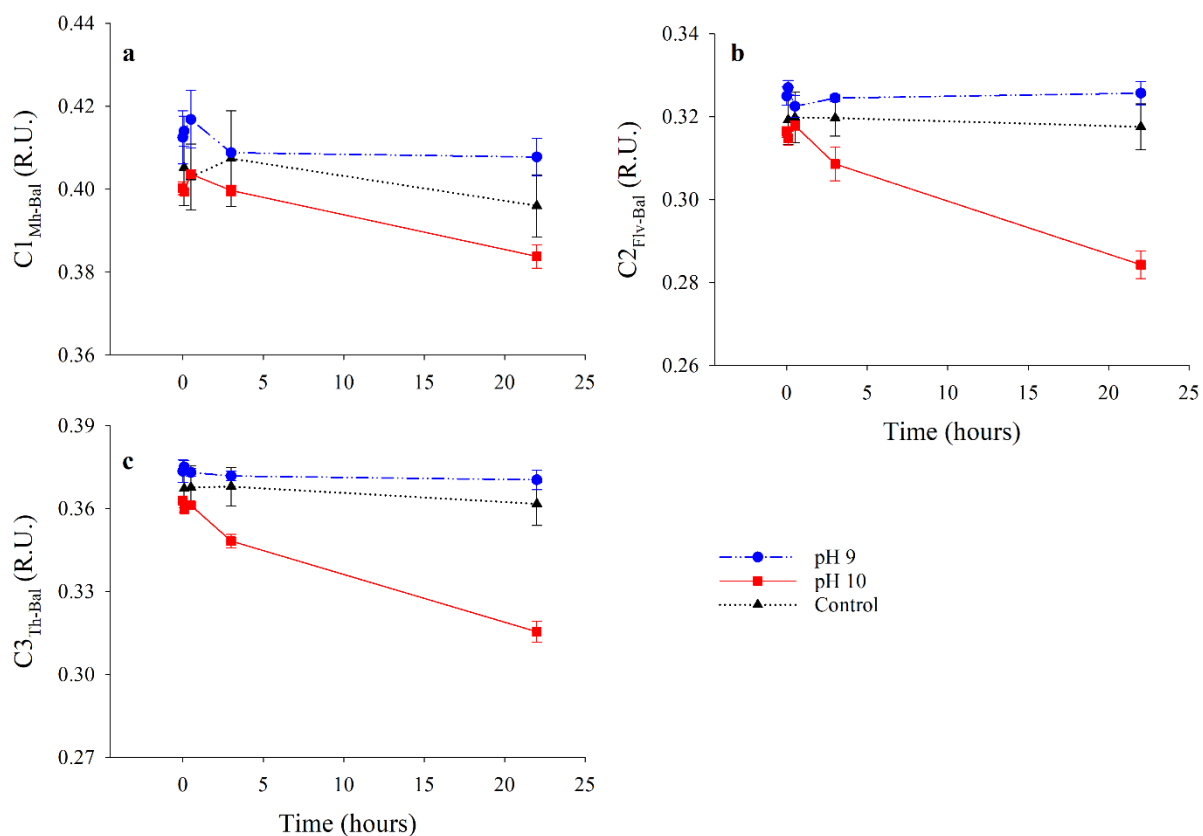
226

227 3.2.3 FDOM fluorescence

228 The PARAFAC validated a 3-component model for the Baltic Sea EEMs experiment (Fig. S2, Tab. S3). Component 1
 229 ($\lambda_{Ex}/\lambda_{Em}$: 290/400 nm, Fig. S2) shows spectroscopic characteristics similar to Coble's peak M ($\lambda_{Ex}/\lambda_{Em}$: 312/[380]420;
 230 Coble (1996)). The comparison with similar components in the OpenFluor database (matches with a TCC > 0.95) allowed
 231 to characterize it as marine humic-like ($C1_{Mh-Bal}$). Component 2 ($\lambda_{Ex}/\lambda_{Em}$: 330/452 nm, Fig. S2) shows spectroscopic
 232 characteristics similar to Coble's peak C ($\lambda_{Ex}/\lambda_{Em}$: 350/451; Coble (1996)). The comparison with similar components in
 233 the OpenFluor database (matches with a TCC > 0.95) allowed to characterize it as Fulvic-like ($C2_{Flv-Bal}$). Component 3
 234 ($\lambda_{Ex}/\lambda_{Em}$: 280/485 nm, Fig. S2) shows spectroscopic characteristics similar to Coble's peak A ($\lambda_{Ex}/\lambda_{Em}$: 260/[380]460 nm;
 235 Coble (1996)). The comparison with similar components in the OpenFluor database (matches with a TCC > 0.95) allowed
 236 to characterize it as Terrestrial humic-like ($C3_{Th-Bal}$).

237 $C1_{Mh-Bal}$ did not show significant changes during the incubation neither in the treatments nor in the control (Fig. 6a, Tab.
 238 S5). $C2_{Flv-Bal}$ did not show significant changes during the incubation at pH 9 and in the control, whereas a decrease of
 239 0.03 R.U. (10%) was observed at pH 10 after 22 hours (Fig. 6b, Tab. S5). $C3_{Th-Bal}$ did not show significant changes during
 240 the incubation at pH 9 and in the control, whereas a decrease of 0.05 R.U. (13%) was observed at pH 10 after 22 hours
 241 (Fig. 6c, Tab. S5).

242



243

244 **Figure 6: Trend of the fluorescent intensity of $C1_{Mh-Bal}$ (a), $C2_{Flv-Bal}$ (b) and $C3_{Th-Bal}$ (c) in the Baltic Sea**
 245 **treatments at pH 9 and 10, and in the control. Error bars refer to the standard deviation among the 3 replicates.**
 246 **Please, note that for some samples the error bars are smaller than the symbols and therefore not visible.**

247

248

249 4 Discussion

250 Even if OAE using alkaline minerals is considered a promising tool to mitigate climate change through the sequestration
 251 and storage of atmospheric CO_2 into the ocean (DOSI, 2022), its impact on the marine ecosystem is still far to be
 252 understood. To the best of our knowledge, this is the first study investigating the potential effects of OAE by hydrated
 253 lime addition on DOM dynamics, with particular regard to DOC concentration and CDOM optical properties. Given the
 254 crucial role that DOM plays in the marine ecosystem, any impact on its dynamics is expected to affect the water quality
 255 and ecosystem functioning through a cascading effect on the microbial loop and the microbial food web.

256

257 4.1 Liming impact on DOM dynamics

258 Our data show the potential effects of hydrated lime addition on DOM dynamics determining a decrease in DOC
 259 concentration (Fig. 1 and 4) and a change in the optical properties of CDOM (Fig. 2, 3, 5 and 6). The decrease in a_{254} , the
 260 increase in $S_{275-295}$ (Fig. 2 and 5) and the decrease in humic-like fluorescence (Fig. 3 and 6) indicate a change in DOM

261 quality with a shift towards molecules with lower average molecular weight and aromaticity degree. These effects are
262 already visible at pH 9, but becomes relevant at pH 10. Different hypotheses can explain our results:

- 263 1) DOM reacts with $\text{Ca}(\text{OH})_2$ and the largest and most aromatic molecules are oxidized to CO_2 ;
- 264 2) the largest and most aromatic molecules adsorb onto primary and secondary carbonate precipitates, that form
265 following the $\text{Ca}(\text{OH})_2$ addition, and sink;
- 266 3) the largest and most aromatic molecules aggregate forming polymer gels or large colloidal material and sink.

267 Interestingly, a significant decrease in DOC concentration was observed only in the unmixed samples at the end of the
268 experiment (22 h after the addition, Fig. 1 and 4), DOC oxidation to CO_2 by reaction with $\text{Ca}(\text{OH})_2$ (hypothesis 1) can
269 therefore be ruled out as a possible removal mechanism. The other 2 hypotheses remain plausible and are supported by
270 the available literature (Conzonno and Cirelli, 1995; Kaushal et al., 2020; Leenheer and Reddy, 2008; Pace et al., 2012).
271 In lake waters, DOM was observed to adsorb onto carbonate particles and co-precipitate with them; the use of CaCO_3
272 precipitation was indeed suggested as an efficient technique for DOM removal during drinking water treatment processes
273 (Leenheer and Reddy, 2008). The mechanism of DOM co-precipitation and/or physical incorporation into CaCO_3 is due
274 to the formation of insoluble calcium. This hypothesis is further supported by the observation of CaCO_3 precipitation
275 following the dissolution of hydrated lime, that was enhanced by the occurrence of nucleation surfaces as particles or
276 solid mineral phases in the solution (Moras et al., 2021).

277 In freshwater ponds, a high affinity of high molecular weight molecules to adsorb onto particles like CaCO_3 was observed
278 by Conzonno and Cirelli (1995) together with a preferential removal of high molecular weight humic substances during
279 CaCO_3 crystals formation. Since humic acids have important environmental functions in controlling the pH and the
280 bioavailability of dissolved metals (Baalousha et al., 2006), their removal may trigger a cascade effect with possible
281 impacts on water quality. Past studies showed that pH per se can affect DOM dynamics as DOM can undergo a fast
282 transition from dissolved to polymer gels (Chin et al., 1998) or large colloidal material (Pace et al., 2012) when pH
283 switches toward more basic values ($\text{pH} > 8$ for seawater).

284 Among the 3 hypotheses mentioned above, the decrease in a_{254} , observed in our experiments, supports the hypothesis 2,
285 suggesting that, following the addition of $\text{Ca}(\text{OH})_2$, the largest and most aromatic dissolved organic molecules adsorb to
286 primary and secondary mineral particles and sink. This hypothesis is further supported by the high removal of the
287 terrestrial components observed in both the Mediterranean Sea ($C_{3\text{Th-Med}}$, -26%) and the Baltic Sea ($C_{3\text{Th-Bal}}$, -13%). This
288 observation agrees with the results of Kaushal et al., (2020) which reported a higher incorporation of the terrestrial humic
289 substances into abiogenically precipitated aragonite, then transferred within coral skeletons, with respect to marine humic
290 substances.

291

292 4.2 Different effects on Mediterranean and Baltic waters

293 The Mediterranean Sea and the Baltic Sea are basins with different biogeochemical characteristics (Tab. 1). Our results
294 show that DOC concentration (Fig. 1 and 4) and a_{254} (Fig. 2 and 5) are 6 and 13 times higher in the Baltic Sea than in the
295 Mediterranean Sea (Tab. 1), these data are consistent with previous studies (Hoikkala et al., 2015; Santinelli, 2015;
296 Santinelli et al., 2010). The lower $S_{275-295}$ (Tab. 1) and the different FDOM composition (Fig. S1 and S2) indicate a higher

297 percentage of terrestrial DOM in the Baltic Sea than in the Mediterranean Sea, as previously reported by Deutsch et al.
298 (2012) and Hoikkala et al. (2015). Indeed, in the Baltic Sea, PARAFAC allowed to characterize humic-like and fulvic-
299 like components but not protein-like ones (Fig. S2, Tab. S4), differently in the Mediterranean Sea the protein-like
300 component was identified (Fig. S1, Tab. S3). Protein-like compounds are usually related to in-situ production, whereas
301 fulvic-like substances mostly have a terrestrial origin. The predominance of terrestrial DOM in the Baltic Sea is due to
302 the high freshwater input from the wide catchment area (~ 4 times as large as the sea itself), and the low seawater input
303 from the North Sea. The Baltic Sea is also characterized by a peculiar carbonate system (Kuliński et al., 2017), exhibiting
304 a wider range of total alkalinity (and pH) compared to the oceans. In particular, the Gulf of Riga, where the water for our
305 experiment was collected, is characterized by a higher total alkalinity and a higher pH with respect to the rest of the Baltic
306 Sea (Beldowski et al., 2010; Kuliński et al., 2017).

307 In our experiments, we observed a different impact of $\text{Ca}(\text{OH})_2$ addition in the Mediterranean Sea and Baltic Sea. In the
308 Mediterranean Sea, a DOC decrease of 6 and 13 μM was recorded at pH 9 and 10, respectively (Tab. S2), indicating a
309 net removal up to 18% of the initial DOC (Fig. 1, Tab. S2). In the Baltic Sea, the maximum removal observed was 6% at
310 pH 10, whereas no effect was recorded at pH 9 (Fig. 4).

311 Even if the salinity, being markedly lower in the Baltic Sea than in the Mediterranean Sea, is probably the main driver of
312 the less pronounced effects on DOM dynamic, it cannot be excluded that the peculiar carbonate system combined with
313 the different concentration and quality of DOM may have influenced the lower removal rates observed in our experiment.
314 The influence of water chemistry is already evident by the 4-times lower amount of $\text{Ca}(\text{OH})_2$ needed to reach pH 9 and
315 10 in the Baltic Sea than in the Mediterranean Sea. Since CaCO_3 precipitation can be one of the main mechanisms
316 explaining our results, the lower amount of $\text{Ca}(\text{OH})_2$ added in the Baltic Sea can explain the lower decrease of DOC
317 observed in this basin than in the Mediterranean Sea. At pH 10, the overall DOC removed in the Baltic Sea is larger (27
318 μM) than in the Mediterranean Sea (11 μM), despite the lower $\text{Ca}(\text{OH})_2$ added. This suggests a removal of 450 μmol of
319 DOC per gram of $\text{Ca}(\text{OH})_2$ added in the Baltic Sea, and 44 μmol of DOC per gram of $\text{Ca}(\text{OH})_2$ added in the
320 Mediterranean Sea. This observation can be explained by the predominance of terrestrial DOM in the Baltic Sea which
321 was suggested to be preferentially removed during abiogenic precipitation of aragonite with respect to marine DOM
322 (Kaushal et al., 2020).

323 It is noteworthy that DOM in the Mediterranean Sea and in the oceans shows a clear seasonal cycle, mostly attributed to
324 the changes in temperature, water stratification and biological activity, affecting DOM concentration, optical properties
325 and stoichiometry (Carlson and Hansell, 2015; Santinelli, 2015; Santinelli et al., 2013). Seasonality strongly affects DOM
326 dynamics also in the Baltic Sea with prevalent allochthonous sources in winter and in-situ production by phytoplankton
327 in spring (Hoikkala et al., 2012; Seidel et al., 2017). Our results, combined with the observed seasonality in DOM
328 dynamics, stress that any plans for liming-based OAE should also take into consideration the season.

329

330 **4.3 Changed DOM dynamics: implication for the marine ecosystems**

331 Our results suggest that CaCO_3 precipitation is the main driver for the sequestration of DOM from the water column. The
332 sinking of the largest and most complex fraction of DOM to the deep oceans could lead to different scenarios.

- 333 1. If the exported DOM is labile (i.e. it is available to microbial removal on the short temporal scale), its export would
334 determine:

- 335 • A depletion of the energy available for heterotrophic prokaryotes in the surface layer, determining a
336 malfunctioning of the microbial loop that could impact the energy transfer to the higher trophic levels. This
337 process could be further enhanced if the primary production is limited by the reduced water transparency
338 due to carbonate formation.
- 339 • The export of energy to the deepest layer (below the carbon compensation depth, CCD), leading to an
340 increased bacterial production, in response to the labile DOM released due to the CaCO₃ dissolution.

341 2. If the exported DOM is refractory (i.e. it is not available to microbial removal on the short temporal scale), it
342 will contribute to C sequestration in the deep waters.

343 Our results indicate the preferential removal of the humic-like fractions by CaCO₃ precipitation. Humic-like substances
344 are considered to constitute the less labile fraction of DOM (Bachi et al., 2023; Zigah et al., 2017) , supporting C
345 sequestration in the deep waters (hypothesis 2) and a change in the lability of DOM in the surface waters, with an increase
346 in the percentage of the labile fraction after CaCO₃ formation. Even if the lability of DOM is a very complex process,
347 depending on a large number of variables (Dittmar et al., 2021), the change in the lability of DOM could be tested in
348 incubation experiments with natural microbial communities collected in the same area as the water used for the
349 experiment. The water for the experiments was filtered through a 0.2 µm filter and it was therefore considered sterile, in
350 order to investigate the potential removal of DOM by microbes, we could inoculate the natural microbial community
351 adding a 10% of unfiltered water from the same site. In order to avoid artefacts from direct pH impacts on the microbial
352 community, before the inoculum the pH should be brought to natural pH by adding HCl.

353 It should also be taken into consideration that the adsorption of DOM onto CaCO₃ particles, itself might reduce the
354 bioavailability, regardless of the inherent properties of the DOM. This process would increase the carbon sequestration
355 into the deep waters, but it would reduce the energy available for the marine ecosystems.

356

357 **5. Conclusions**

358 This study reports the first evidence of the potential effects of OAE on DOM dynamics in two contrasting environments:
359 the oligotrophic Mediterranean Sea, known for its low DOC concentration, and the eutrophic Baltic Sea, characterized by
360 high DOM concentration mostly of terrestrial origin. Our findings suggest that ocean alkalization by Ca(OH)₂ sparging
361 may alter DOM dynamics and, consequently, have a potential impact on the entire marine ecosystem. To mitigate these
362 effects, it is crucial to reduce the duration and intensity of pH spikes, ensuring they remain below the safety threshold of
363 pH 9. We stress the need to take into consideration the physico-chemical properties (e.g. salinity, pH, DOM concentration
364 and quality) of the basin and the season, to efficiently manage ocean liming and mitigate the potential impacts of ocean
365 alkalization on DOM pool.

366 Although the experimental conditions used in this study were more severe than actual liming practices, where the release
367 of Ca(OH)₂ in the ship's wake undergoes rapid dilution that significantly reduces pH changes, our results provide new
368 insights into the possible impacts due to physico-chemical processes.

369 It is important to highlight that the experiments in this study were conducted using sterilized seawater, thus excluding the
370 potential interplay of biological processes on DOM dynamics. To gain a more comprehensive understanding of possible
371 OAE impacts, future research should address the influence of biological processes, as well as factors like dilution rates,
372 water mixing, and realistic durations and severities of pH peaks. Scaling up the experimental setup to mesocosms would

373 allow for repeated additions and longer observation periods, enabling a more accurate representation of real-world
374 conditions.

375

376 **Author contribution**

377 Conceptualization by CS, DB and AA. CS designed and supervised the experiments and SV, RBS, GB, GC, MG carried them out.

378 Funding acquisition by SC and AA. CS prepared the manuscript with contributions from all co-authors.

379

380 **Competing interests**

381 The authors declare that they have no conflict of interest.

382

383 **Acknowledgements**

384 The current study has received funding from European Lime Association (EuLA) through a research contract established with CoNISM
385 (National Inter-University Consortium for Marine Sciences) in Italy. We warmly thank Roberto Moreschi and Dario Ravasio
386 (UNICALCE Sedrina) for kindly sending the samples of Ca-hydroxide used for our experiments. We thank Giovanni Cappello
387 (Limenet) and Agija Bistere (Hyrogas) for sampling and sending to Pisa the Baltic Sea seawater. The authors are grateful to Marco
388 Carloni and Valtere Evangelista for their support in sampling of Mediterranean Sea water and CDOM/FDOM analyses and to Rosanna
389 Cascone, Rosanna Claps and Claudia Neri, (IBF-CNR, Italy) for the assistance in the financial management. The authors wish to thank
390 Aurela Shitza and Marlena Wissel from EuLA for their valuable feedback and helpful suggestions which greatly contributed to the
391 overall improvement of this paper.

392

393 **References**

- 394 Baalousha, M., Kammer, F. V. D., Motelica-Heino, M., Hilal, H. S., and Le Coustumer, P.: Size
395 fractionation and characterization of natural colloids by flow-field flow fractionation coupled to multi-angle
396 laser light scattering, *J Chromatogr A*, 1104, 272–281, <https://doi.org/10.1016/j.chroma.2005.11.095>, 2006.
- 397 Bachi, G., Morelli, E., Gonnelli, M., Balestra, C., Casotti, R., Evangelista, V., Repeta, D. J., and Santinelli,
398 C.: Fluorescent properties of marine phytoplankton exudates and lability to marine heterotrophic prokaryotes
399 degradation, *Limnol Oceanogr*, 68, 982–1000, <https://doi.org/10.1002/lno.12325>, 2023.
- 400 Beldowski, J., Löffler, A., Schneider, B., and Joensuu, L.: Distribution and biogeochemical control of total
401 CO₂ and total alkalinity in the Baltic Sea, *Journal of Marine Systems*, 81, 252–259,
402 <https://doi.org/10.1016/j.jmarsys.2009.12.020>, 2010.
- 403 Butenschön, M., Lovato, T., Masina, S., Caserini, S., and Grosso, M.: Alkalinization Scenarios in the
404 Mediterranean Sea for Efficient Removal of Atmospheric CO₂ and the Mitigation of Ocean Acidification,
405 *Frontiers in Climate*, 3, 614537, <https://doi.org/10.3389/fclim.2021.614537>, 2021.
- 406 Calvin, K., Dasgupta, D., Krinner, G., Mukherji, A., Thorne, P. W., Trisos, C., Romero, J., Aldunce, P.,
407 Barrett, K., Blanco, G., Cheung, W. W. L., Connors, S., Denton, F., Diongue-Niang, A., Dodman, D.,
408 Garschagen, M., Geden, O., Hayward, B., Jones, C., Jotzo, F., Krug, T., Lasco, R., Lee, Y.-Y., Masson-
409 Delmotte, V., Meinshausen, M., Mintenbeck, K., Mokssit, A., Otto, F. E. L., Pathak, M., Pirani, A.,
410 Poloczanska, E., Pörtner, H.-O., Revi, A., Roberts, D. C., Roy, J., Ruane, A. C., Skea, J., Shukla, P. R.,
411 Slade, R., Slangen, A., Sokona, Y., Sörensson, A. A., Tignor, M., van Vuuren, D., Wei, Y.-M., Winkler, H.,
412 Zhai, P., Zommers, Z., Hourcade, J.-C., Johnson, F. X., Pachauri, S., Simpson, N. P., Singh, C., Thomas, A.,
413 Totin, E., Alegría, A., Armour, K., Bednar-Friedl, B., Blok, K., Cissé, G., Dentener, F., Eriksen, S., Fischer,
414 E., Garner, G., Guivarch, C., Haasnoot, M., Hansen, G., Hauser, M., Hawkins, E., Hermans, T., Kopp, R.,
415 Leprince-Ringuet, N., Lewis, J., Ley, D., Ludden, C., Niamir, L., Nicholls, Z., Some, S., Szopa, S., Trewin,
416 B., van der Wijst, K.-I., Winter, G., Witting, M., Birt, A., and Ha, M.: IPCC, 2023: Climate Change 2023:
417 Synthesis Report. Contribution of Working Groups I, II and III to the Sixth Assessment Report of the
418 Intergovernmental Panel on Climate Change [Core Writing Team, H. Lee and J. Romero (eds.)]. IPCC,
419 Geneva, Switzerland., <https://doi.org/10.59327/IPCC/AR6-9789291691647>, 2023.
- 420 Camatti, E., Valsecchi, S., Caserini, S., Barbaccia, E., Santinelli, C., Basso, D., and Azzellino, A.: Short-term
421 impact assessment of ocean liming: A copepod exposure test, *Mar Pollut Bull*, 198, 115833,
422 <https://doi.org/10.1016/j.marpolbul.2023.115833>, 2024.
- 423 Carlson, C. A. and Hansell, D. A.: DOM Sources, Sinks, Reactivity, and Budgets, in: *Biogeochemistry of*
424 *Marine Dissolved Organic Matter*, 65–126, <https://doi.org/10.1016/B978-0-12-405940-5.00003-0>, 2015.
- 425 Caserini, S., Pagano, D., Campo, F., Abbà, A., De Marco, S., Righi, D., Renforth, P., and Grosso, M.:
426 Potential of Maritime Transport for Ocean Liming and Atmospheric CO₂ Removal, *Frontiers in Climate*, 3,
427 575900, <https://doi.org/10.3389/fclim.2021.575900>, 2021.
- 428 Chikamoto, M. O., DiNezio, P., and Lovenduski, N.: Long-Term Slowdown of Ocean Carbon Uptake by
429 Alkalinity Dynamics, *Geophys Res Lett*, 50, <https://doi.org/10.1029/2022GL101954>, 2023.
- 430 Chin, W.-C., Orellana, M. V., and Verdugo, P.: Spontaneous assembly of marine dissolved organic matter
431 into polymer gels, *Nature*, 391, 568–572, <https://doi.org/10.1038/35345>, 1998.
- 432 Coble, P.: Characterization of marine and terrestrial DOM in seawater using excitation-emission matrix
433 spectroscopy, *Mar Chem*, 51, 325–346, 1996.
- 434 Conzonno, V. H. and Cirelli, A. F.: Dissolved organic matter in Chascomus Pond (Argentina). Influence of
435 calcium carbonate on humic acid concentration, *Hydrobiologia*, 297, 55–59,
436 <https://doi.org/10.1007/BF00033501>, 1995.

437 Del Vecchio, R. and Blough, N. V.: Spatial and seasonal distribution of chromophoric dissolved organic
438 matter and dissolved organic carbon in the Middle Atlantic Bight, in: *Marine Chemistry*, 169–187,
439 <https://doi.org/10.1016/j.marchem.2004.02.027>, 2004.

440 Deutsch, B., Alling, V., Humborg, C., Korth, F., and Mörtz, C. M.: Tracing inputs of terrestrial high
441 molecular weight dissolved organic matter within the Baltic Sea ecosystem, *Biogeosciences*, 9, 4465–4475,
442 <https://doi.org/10.5194/bg-9-4465-2012>, 2012.

443 Dittmar, T., Lennartz, S. T., Buck-Wiese, H., Hansell, D. A., Santinelli, C., Vanni, C., Blasius, B., and
444 Hehemann, J.-H.: Enigmatic persistence of dissolved organic matter in the ocean, *Nat Rev Earth Environ*, 2,
445 570–583, <https://doi.org/10.1038/s43017-021-00183-7>, 2021.

446 DOSI: Ocean Alkalinity Enhancement Deep Ocean Stewardship Initiative Policy Brief, 2022.

447 Gattuso, J.-P., Mach, K. J., and Morgan, G.: Ocean acidification and its impacts: an expert survey, *Clim*
448 *Change*, 117, 725–738, <https://doi.org/10.1007/s10584-012-0591-5>, 2013.

449 González, M. F. and Ilyina, T.: Impacts of artificial ocean alkalization on the carbon cycle and climate in
450 Earth system simulations, *Geophys Res Lett*, 43, 6493–6502, <https://doi.org/10.1002/2016GL068576>, 2016.

451 Gore, S., Renforth, P., and Perkins, R.: The potential environmental response to increasing ocean alkalinity
452 for negative emissions, *Mitig Adapt Strateg Glob Chang*, 24, 1191–1211, [https://doi.org/10.1007/s11027-](https://doi.org/10.1007/s11027-018-9830-z)
453 018-9830-z, 2019.

454 Hansell, D., Carlson, C., Repeta, D., and Schlitzer, R.: Dissolved Organic Matter in the Ocean: A
455 Controversy Stimulates New Insights, *Oceanography*, 22, 202–211,
456 <https://doi.org/10.5670/oceanog.2009.109>, 2009.

457 Hansell, D. A.: Dissolved Organic Carbon Reference Material Program, *Eos, Transactions American*
458 *Geophysical Union*, 86, 318, <https://doi.org/10.1029/2005EO350003>, 2005.

459 Heinze, C., Meyer, S., Goris, N., Anderson, L., Steinfeldt, R., Chang, N., Le Quéré, C., and Bakker, D. C. E.:
460 The ocean carbon sink – impacts, vulnerabilities and challenges, *Earth System Dynamics*, 6, 327–358,
461 <https://doi.org/10.5194/esd-6-327-2015>, 2015.

462 Helms, J. R., Stubbins, A., Ritchie, J. D., Minor, E. C., Kieber, D. J., and Mopper, K.: Absorption spectral
463 slopes and slope ratios as indicators of molecular weight, source, and photobleaching of chromophoric
464 dissolved organic matter, *Limnol Oceanogr*, 53, 955–969, <https://doi.org/10.4319/lo.2008.53.3.0955>, 2008.

465 Hinga, K.: Effects of pH on coastal marine phytoplankton, *Mar Ecol Prog Ser*, 238, 281–300,
466 <https://doi.org/10.3354/meps238281>, 2002.

467 Hoikkala, L., Lahtinen, T., Perttilä, M., and Lignell, R.: Seasonal dynamics of dissolved organic matter on a
468 coastal salinity gradient in the northern Baltic Sea, *Cont Shelf Res*, 45, 1–14,
469 <https://doi.org/10.1016/j.csr.2012.04.008>, 2012.

470 Hoikkala, L., Kortelainen, P., Soenne, H., and Kuosa, H.: Dissolved organic matter in the Baltic Sea, *Journal*
471 *of Marine Systems*, 142, 47–61, <https://doi.org/10.1016/j.jmarsys.2014.10.005>, 2015.

472 Kaushal, N., Yang, L., Tanzil, J. T. I., Lee, J. N., Goodkin, N. F., and Martin, P.: Sub-annual fluorescence
473 measurements of coral skeleton: relationship between skeletal luminescence and terrestrial humic-like
474 substances, *Coral Reefs*, 39, 1257–1272, <https://doi.org/10.1007/s00338-020-01959-x>, 2020.

475 Kheshgi, H. S.: Sequestering atmospheric carbon dioxide by increasing ocean alkalinity, *Energy*, 20, 915–
476 922, [https://doi.org/10.1016/0360-5442\(95\)00035-F](https://doi.org/10.1016/0360-5442(95)00035-F), 1995.

477 Kuliński, K., Schneider, B., Szymczycha, B., and Stokowski, M.: Structure and functioning of the acid–base
478 system in the Baltic Sea, *Earth System Dynamics*, 8, 1107–1120, <https://doi.org/10.5194/esd-8-1107-2017>,
479 2017.

480 Lawaetz, A. J. and Stedmon, C. A.: Fluorescence intensity calibration using the Raman scatter peak of water,
481 *Appl Spectrosc*, 63, 936–940, <https://doi.org/10.1366/000370209788964548>, 2009.

482 Leenheer, J. A. and Reddy, M. M.: Co-precipitation of dissolved organic matter by calcium carbonate in
483 pyramid lake, nevada, *Annals of Environmental Science*, 2008.

484 Moras, P., Menteş, T. O., Schiller, F., Ferrari, L., Topwal, D., Locatelli, A., Sheverdyeva, P. M., and
485 Carbone, C.: Reference plane for the electronic states in thin films on stepped surfaces, *Phys Rev B*, 103,
486 165426, <https://doi.org/10.1103/PhysRevB.103.165426>, 2021.

487 Murphy, K. R., Stedmon, C. A., Graeber, D., and Bro, R.: Fluorescence spectroscopy and multi-way
488 techniques. *PARAFAC, Analytical Methods*, 5, 6557, <https://doi.org/10.1039/c3ay41160e>, 2013.

489 Murphy, K. R., Stedmon, C. A., Wenig, P., and Bro, R.: OpenFluor- an online spectral library of auto-
490 fluorescence by organic compounds in the environment, *Analytical Methods*, 6, 658–661,
491 <https://doi.org/10.1039/C3AY41935E>, 2014.

492 Omanović, D., Santinelli, C., Marcinek, S., and Gonnelli, M.: ASFit - An all-inclusive tool for analysis of
493 UV–Vis spectra of colored dissolved organic matter (CDOM), *Comput Geosci*, 133, 104334,
494 <https://doi.org/10.1016/j.cageo.2019.104334>, 2019.

495 Omanović, D., Marcinek, S., and Santinelli, C.: TreatEEM—A Software Tool for the Interpretation of
496 Fluorescence Excitation-Emission Matrices (EEMs) of Dissolved Organic Matter in Natural Waters, *Water*
497 (Basel), 15, 2214, <https://doi.org/10.3390/w15122214>, 2023.

498 Pace, M. L., Reche, I., Cole, J. J., Fernández-Barbero, A., Mazuecos, I. P., and Prairie, Y. T.: pH change
499 induces shifts in the size and light absorption of dissolved organic matter, *Biogeochemistry*, 108, 109–118,
500 <https://doi.org/10.1007/s10533-011-9576-0>, 2012.

501 Royal Society and Royal Academy of Engineering: Greenhouse Gas Removal, 2018.

502 Santinelli, C.: DOC in the Mediterranean Sea, in: *Biogeochemistry of Marine Dissolved Organic Matter*,
503 edited by: Hansell, D. A., Elsevier, 579–608, <https://doi.org/10.1016/B978-0-12-405940-5.00013-3>, 2015.

504 Santinelli, C., Nannicini, L., and Seritti, A.: DOC dynamics in the meso and bathypelagic layers of the
505 Mediterranean Sea, *Deep Sea Research Part II: Topical Studies in Oceanography*, 57, 1446–1459,
506 <https://doi.org/10.1016/j.dsr2.2010.02.014>, 2010.

507 Santinelli, C., Hansell, D. A., and Ribera d’Alcalà, M.: Influence of stratification on marine dissolved
508 organic carbon (DOC) dynamics: The Mediterranean Sea case, *Prog Oceanogr*, 119, 68–77,
509 <https://doi.org/10.1016/j.pocean.2013.06.001>, 2013.

510 Santinelli, C., Follett, C., Retelletti Brogi, S., Xu, L., and Repeta, D.: Carbon isotope measurements reveal
511 unexpected cycling of dissolved organic matter in the deep Mediterranean Sea, *Mar Chem*, 177, 267–277,
512 <https://doi.org/10.1016/j.marchem.2015.06.018>, 2015.

513 Seidel, M., Manecki, M., Herlemann, D. P. R., Deutsch, B., Schulz-Bull, D., Jürgens, K., and Dittmar, T.:
514 Composition and Transformation of Dissolved Organic Matter in the Baltic Sea, *Front Earth Sci (Lausanne)*,
515 5, <https://doi.org/10.3389/feart.2017.00031>, 2017.

516 Weishaar, J., Aiken, G., Bergamaschi, B., Fram, M., Fujii, R., and Mopper, K.: Evaluation of specific ultra-
517 violet absorbance as an indicator of the chemical content of dissolved organic carbon, *Environ Sci Technol*,
518 37, 4702–4708, <https://doi.org/10.1021/es030360x>, 2003.

519 Zigah, P. K., McNichol, A. P., Xu, L., Johnson, C., Santinelli, C., Karl, D. M., and Repeta, D. J.:
520 Allochthonous sources and dynamic cycling of ocean dissolved organic carbon revealed by carbon isotopes,
521 *Geophys Res Lett*, 44, 2407–2415, <https://doi.org/10.1002/2016GL071348>, 2017.

522